mission analysis, including Earth's mask for a space telescope, scan of the apparent Earth by an infrared sensor, and a scan of the stars combined with other mission constraints. Following are two applications of this representation.

Geometrical Limitations on Attitude Determination of a Spinning Spacecraft

The study is restricted to the case of a spacecraft located at synchronous altitude with a spin axis in the equatorial region. The infrared sensor gives the Sun-spin axis-to-Earth rotation angle Ψ, the Earth half-width angle Λ, and the Sun angle β. This information can be used to determine the location of the spin axis direction in at least two ways.[1] To illustrate the inertial coordinate representation, the analysis will be restricted as follows: the spin axis A is at distance β from the Sun and thus on a circle Θ of center H and radius β. The on-board sensors are of limited accuracy, and the angles β, Ψ are known with some uncertainty. Curves Θ and Ψ should be replaced by strips, and the spin axis is located at the intersection of two strips somewhere inside a distorted parallelogram. A plane representation of the celestial sphere is chosen with α along the x axis and declination δ along the y axis. As the quantities β and Ψ are calculated in the (α, δ) coordinate system, curves Θ of constant β values and curves of constant Ψ are plotted. Figure 2 represents the geometry of the intersection. The strips in Θ and Ψ are obtained by tracing curves corresponding to the upper and lower limits for each variable. The Sun elevation angle β is known with a good accuracy, and the width of the strip is almost negligible. On the other hand, Ψ is known with some error, and the strip is quite wide in the equatorial region. The parallelogram reduces to a segment AB significantly elongated in declination; the inertial coordinate representation immediately yields the uncertainty to be expected in the attitude determination for an inertial platform. Figure 2 can be compared to Fig. 10-8 of Ref. 1. When compared to the figure from Ref. 1, the segment from this Note would be a portion of a parallel of the local sphere centered on the spacecraft with the Sun located at the North Pole. However, our figure gives results directly in inertial coordinates, which is not the case of Fig. 10-8.

Earth-Mask Viewing Constraint for a Space Telescope

The case of an inertial space platform in a circular high inclination orbit is also considered. It can be readily seen from Fig. 3 that in one orbit the apparent Earth sweeps a band of the celestial sphere. If α_N is the right ascension of the ascending node and i the inclination of the orbit, the location of the pole of the orbit will be $\alpha_P = \alpha_N - \pi/2$, $\delta_P = \pi/2 - i$. The boundaries of the Earth-mask path are defined by their elevation angles θ_i, θ_s counted from axis OP. If the space telescope orientation θ_T as measured from OP is such that $\theta_i < \theta_T < \theta_s$, the space telescope will suffer a partial eclipse. As time elapses, the pole of the orbit moves on a parallel, and our representation conditions of eclipse can be obtained easily. Furthermore, additional constraints on star or Sun sensors can be handled with the same representation. For example, the crude attitude determination of the French-Soviet experiment Sigma is obtained with a bright-star-large-field-of-view sensor and a slit Sun sensor. Solution in celestial coordinates can be obtained easily since all the necessary information is expressed in celestial coordinates.

Reference

[1]Chen, L.C. and Wertz, J.R., "Geometrical Basis of Attitude Determination," *Spacecraft Attitude Determination and Control*, D. Reidel Publishing Co., Dordrecht, The Netherlands, 1978, pp. 343-361.

Roll Damping of Cruciform-Tailed Missiles

Donald W. Eastman*
Boeing Aeospace Company, Seattle, Washington

Nomenclature

C_ℓ	= rolling moment coefficient, rolling moment/qSD
C_{ℓ_p}	= roll damping coefficient, $\partial C_\ell / \partial (pD/2V)$
C_{ℓ_δ}	= rolling moment due to cant of tail surfaces, $\partial C_\ell / \partial \delta$
D	= reference length
M	= freestream Mach number
p	= roll rate, rad/s
$(pD/2V)$	= reduced frequency
q	= freestream dynamic pressure
S	= reference area
V	= freestream velocity
Y_{CENT}	= radial distance from body centerline to centroid of area of exposed tail fin
δ	= cant angle of one fin (all fins deflected uniformly), rad

Introduction

A simple method for predicting roll damping derivatives of cruciform-tailed missiles is presented here. The method is based on an empirical correlation of experimenal data for several cruciform-tailed missiles,[1-8] at Mach numbers from 0 to 4.0. Its use is limited to small angles of attack.

Prediction Method

Configurations for which experimental data were correlated are shown at the top of Fig. 1. Roll damping is correlated in Fig. 1 with the rolling moment due to tail cant angle and the distance from the missile centerline to the centroid of the exposed fin area. The dashed line represents the approximate average of much data for the Basic Finner missile. The Boeing missile was tested with five different sets of fins. The range and average of results for the five configurations are shown. Based on this correlation, the following equation can be used to predict roll damping.

$$C_{\ell_p} = -2.15 (Y_{\text{CENT}}/D) C_{\ell_\delta} \tag{1}$$

For this equation to be valid, the roll rate reduced frequency $(pD/2V)$ must include the number 2, and the same reference length must be used for the rolling moment coefficient and reduced frequency.

The type of correlation shown in Fig. 1 is not new. Bolz and Nicolaides[1] used supersonic linearized theory to predict $(C_{\ell_p}/C_{\ell_\delta})$ for the Basic Finner missile and compared predictions with experimental data. Adams and Dugan,[9] using slender body theory, predicted that $(C_{\ell_p}/C_{\ell_\delta})$ was a function of the ratio of body diameter to tail span. However, the experimental data in Fig. 1 would not correlate using the correlation curve developed by them.

Introduction of the empirical term (Y_{CENT}/D) provides an excellent correlation of roll damping data for a wide range of

Received Oct. 29, 1984; revision received Feb. 20, 1985.

*Senior Principal Engineer, Flight Technology Organization. Member AIAA.

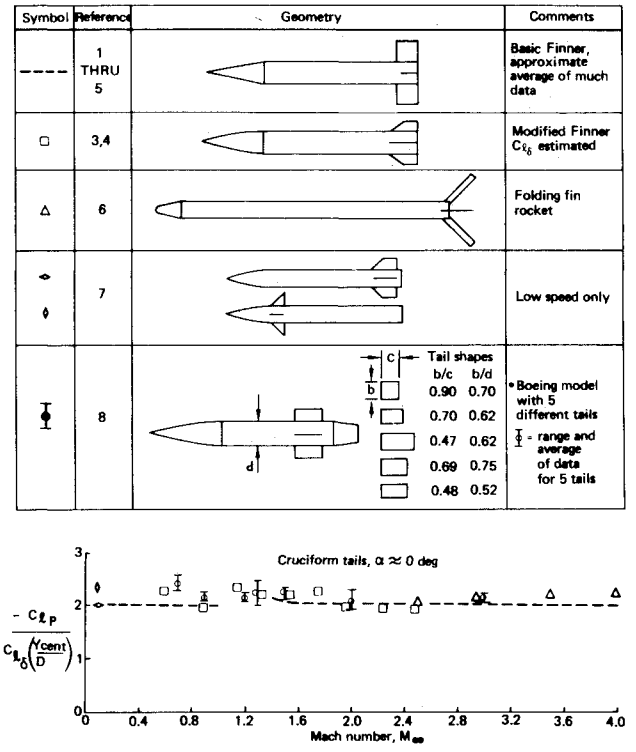

Fig. 1 Correlation of roll damping data for cruciform-tailed missiles.

configurations. This term is intended to account for differences in tail geometry and the ratio of body diameter to tail span. To obtain C_{ℓ_p} from Fig. 1, C_{ℓ_δ} must be known. Theoretial methods[10] and much experimental data are available for predicting this coefficient. Figure 1 is valid only for a missile with a single set of cruciform fins. If canards or wings are located ahead of a tail, large roll damping interference effects may occur between the forward and aft surfaces.[2]

Use of Eq. (1) to predict roll damping, within the limitations discussed above, should be adequate for most engineering purposes. Figure 1 should be updated as additional experimental data become available.

References

[1]Bolz, R.E. and Nicolaides, J.D., "A Method of Determining Some Aerodynamic Coefficients from Supersonic Free-Flight Tests of a Rolling Missile," *Journal of the Aerospace Sciences,* Vol. 17, Oct. 1950, pp. 609-621.

[2]Nicolaides, J.D. and Bolz, R.E., "On the Pure Rolling Motion of Winged and/or Finned Missiles in Varying Supersonic Flight," *Journal of the Aerospace Sciences,* Vol. 20, March 1953, pp. 160-168.

[3]Oberkampf, W.L., "Prediction of Roll Moments on Finned Bodies in Supersonic Flow," *Journal of Spacecraft and Rockets,* Vol. 12, Jan. 1975, pp. 17-21.

[4]Uselton, B.L. and Jenke, L.M., "Experimental Missile Pitch- and Roll-Damping Characteristics at Large Angles of Attack," *Journal of Spacecraft and Rockets,* Vol. 14, April 1977, pp. 241-247.

[5]Murthy, H.S., "Subsonic and Transonic Roll Damping Measurements on Basic Finner," *Journal of Spacecraft and Rockets,* Vol. 19, Jan.-Feb. 1982, pp. 86-87.

[6]Uselton, J.C. and Carman, J.B., "Wind Tunnel Investigation of the Roll Characteristics of the Improved 2.75-inch-Diameter Folding Fin Aircraft Rocket at Mach Numbers from 2.5 to 4.5," Arnold Engineering Development Center, Arnold Air Force Station, TN, AEDC-TR-69-207, 1969.

[7]Hardy, S.R., "Nonlinear Rolling Motion Analysis of a Canard Controlled Missile Configuration at Angles of Attack from 0 to 30 Degrees in Incompressible Flow," Naval Surface Weapons Center, Dahlgren, VA, NSW/DL-TR-3808, 1978.

[8]Monk, J.R. and Phelps, E.R., "GSRS Aerodynamic Analysis Report," Boeing Aerospace Co., Seattle, WA, D328-10055-1, 1978.

[9]Adams, G.J. and Dugan, D.W., "Theoretical Damping in Roll and Rolling Moment Due to Differential Wing Incidence for Slender Cruciform Wings and Wing-Body Combination," NACA 1088, 1958.

[10]Prakash, S. and Khurana, D.D., "A Simple Estimation Procedure of Roll-Rate Derivatives for Finned Vehicles," *Journal of Spacecraft and Rockets,* Vol. 21, May-June 1984, pp. 318-320.

A Calorimetric Bomb for Determining Heats of Combustion of Hypergolic Propellants

S.R. Jain* and G. Rajendran†
Indian Institute of Science, Bangalore, India

Introduction

In connection with our studies on hypergolic hybrid propellant systems,[1-3] it was found desirable to have an idea of the actual experimental values of their heats of combustion. A survey of the literature showed that, although a variety of bomb calorimeters[4,5] are available for measuring the heat of combustion values of solid fuels in gaseous oxygen, no suitable device exists so far for determining these values using a liquid oxidizer instead of oxygen. The apparatus described by Rastogi and Kishore[6] gives values very much lower than expected. Herein we report the design and operation of an improved bomb-calorimetric device for measuring the heats of combustion of hypergolic hybrid and biliquid propellant systems.

Experimental

Bomb Calorimetric Device

The usual pressure bomb assembly for the calorimetric measurements has been modified as shown in Fig. 1. The liquid oxidizer is placed in a specially designed duck-shaped glass vessel. The glass duck is supported by two loops of a stainless steel (SS) wire hanger around the pegs at the sides so that it is able to rotate freely. The hanger in turn is fixed by means of a screw to the lid of the bomb. The fuse wire usually meant for igniting the fuel is used for keeping the glass duck in the upright position, instead.

To start with, a known amount of the liquid oxidizer (HNO_3) is placed in the glass duck which is then fixed onto the hanger and supported by the fuse wire in the upright position. The fuel is placed in the SS cup. The bomb is then carefully closed and kept in an isothermal static-bomb calorimeter while connected to the firing unit. After the initial temperature has been noted, the firing switch is pressed, which results in the snapping of the fuse wire. The duck inverts and pours the entire oxidizer onto the fuel causing instantaneous ignition of the fuel. The rise in temperature is then noted and the heat of combustion is calculated[7] from the rise in temperature and water equivalent data. The water equivalent of the calorimeter was determined by the usual procedure in oxygen using AR-grade benzoic acid. The experiments were repeated for each fuel, varying the amount of the oxidizer close to

Received April 25, 1984; revision received June 15, 1984.

*Professor, Department of Aerospace Engineering.
†Ph.D. Student, Department of Inorganic and Physical Chemistry.